Quantum Computation
for Hypersonic Chemistry and Materials

Charles Chung[1], Triet Friedhoff[1], Mariana LaDue[1], Courtney Long[1], Paul Parazzoli[1], Thomas Ward[1],
Igor Alvarado[2], Michael Brown[3], Amit Surana[4], and Bob Dirgo[5]

[1]IBM Quantum — [2]Collins Aerospace — [3]Aerospace Systems Directorate, Air Force Research Lab —
[4]RTX Technology Research Center — [5]Ohio Aerospace Institute

April 24, 2025

Contents

1 Executive Summary

This report provides a perspective on the application of quantum computers to hypersonic platform development, discussing hypersonic chemistry and materials, in general, and in particular, focusing on hypersonic atmospheric thermochemistry.

Quantum simulation of hypersonic atmospheric thermochemistry by solving the Schrödinger equation, the quantum generalization of Newton's Second Law, for hypersonic chemical reactions is identified as a near-term opportunity that has the potential to improve the accuracy of and increase confidence in classical hypersonic fluid simulations that are difficult to verify experimentally. This paper conducts diligence on this opportunity and concludes that initial quantum computations are feasible on currently available quantum computers. Investment will be required to realize this opportunity to secure resources in people, time, and access to quantum computers.

This use case can also serve a second purpose of establishing confidence in quantum computers as a new technology for the aerospace industry for more advanced quantum applications that are beyond the capabilities of classical computers to verify, such as the simulation of advanced aerospace materials.

A characteristic of hypersonic flight is that the temperatures at leading airframe edges can exceed 2,000 K which causes the atmospheric gases around the airframe to undergo chemical reactions. Atmospheric reactions directly impact vehicle performance, such as by changing air composition, lift and drag forces, surface temperatures, and airframe degradation rates.

Due to the high temperatures, there are a number of chemistry and materials challenges to developing hypersonic platforms, such as modeling atmospheric chemical reactions, hypersonic propulsion combustion, and high temperature, high strength-to-weight structural and thermal barrier materials.

Given the extreme conditions, empirical approaches to hypersonic development are notoriously challenging, demanding substantial time and financial resources. Classical computational methods offer the potential to accelerate development; however, they face inherent limitations in simulating the complex chemistry and fluid flows characteristic of hypersonic environments.

Quantum computers emerge as a promising technology, offering the potential for improved accuracy and reduced runtimes compared to classical approaches *for some applications.* Chemical and material simulation is the likely nearest-term application for quantum computers. Other application areas include machine learning, combinatorial optimization, and linear algebra. Quantum computing for computational fluid dynamics is a potential longer-term application and is a current area of active research.

The capabilities of quantum computers naturally align with the quantum nature of chemistry and materials. Solving the Schrödinger equation exemplifies this capability. For classical computers, the computational complexity for solving the Schrödinger equation grows exponentially with system size, rendering the simulation of larger systems intractable. In contrast, the computational complexity for quantum computers exhibits a much slower polynomial growth[2], making the simulation of larger systems tractable.

Given that N_2 and O_2 constitute 99% of the atmosphere at sea level, reactions involving these species are critical for understanding hypersonic aerodynamics. Accurately modeling the breaking of N_2 triple bonds and O_2 double bonds necessitates accounting for the multi-reference nature of dissociation and high degrees of electron correlation. The accuracy of these chemical models directly impacts the accuracy of hypersonic fluid flow simulations, with discrepancies in chemical models leading to temperature variations of hundreds to thousands of Kelvin, affecting air composition, lift and drag, airframe heat flux, material degradation rates, and many other effects. Notably, N_2 dissociation rate constants exhibit an order of magnitude uncertainty across hypersonic thermochemistry models within relevant temperature ranges.[37]

Modeling reactions with N_2 and O_2 is within the capabilities of near-term quantum computers, as evidenced by early quantum computations of the N_2 potential energy curve demonstrated in 2024.[36] Among the most challenging reactions to model is the $N_2 + N_2 = N_2 + 2N$ reaction (referred to as the N_4 reaction)[3]. Feasibility assessments for simulating the N_4 reaction with minimal basis sets place a lower bound on qubit counts at 32 and 2-qubit gate counts at 788. This is within the capabilities of current quantum computers, which have 156 qubits and can execute 5,000 2-qubit gates.

For larger, more accurate basis sets, such as cc-pVDZ[9], 104 qubits and approximately 7,000 2-qubit gates are required. And for the aug-cc-pVDZ basis, 176 qubits and approximately 18,000 2-qubit gates are required. However, these estimates are for the full chemical active space (minus the core orbitals, which are frozen since they do not participate in the reaction). As a point of comparison, the current classical state-of-the-art is the University of Minnesota (UMN) potential energy surface (PES), which uses the maug-cc-pVDZ basis in a 12-orbital space.

Quantum computers are expected to be able to handle larger spaces, which can result in more accurate calculations. Already, calculations in a space of 26 orbitals have been demonstrated on quantum computers. This opens the possibility of a more accurate simulation of the N_4 reaction in the same basis, but within a larger space, which in turn, can result in more accurate hypersonic fluid simulations. This could be impactful because PES's are not directly empirically verifiable and they are often one of the largest sources of error to the inputs of the hypersonic fluid simulation. However, while the size of active space can be an important determinant in accuracy, it is only one factor among many, so improved accuracies cannot be guaranteed. An opportunity for investment is to execute the N_4 PES computation on a quantum computer to evaluate if greater accuracy is achievable.

In the IBM Quantum roadmap (Figure 8), quantum computers with 1,092 qubits are expected in 2025. And, the upper limit of 2-qubit gate operations is expected to triple by 2028 to 15,000 operations. Then in 2029, quantum error correction is expected to become available, and the 2-qubit gate count is expected jump to 100 M operations on 200 logical qubits.

Although current quantum computers with more qubits and 2-qubit gates are expected, before quantum error correction is available, algorithmic limitations and signal-to-noise ratio degradation effectively restrict practical computations on quantum computers to approximately 60-70 qubits, regardless of hardware size. As a result, before 2029, when error correction is expected, this algorithmic ceiling means that even as quantum hardware continues to advance—with increased qubit counts and 2-qubit gate counts — the practical ability to model complex reactions like N_4 will depend not just on hardware improvements but on corresponding algorithmic advances that maintain sufficient signal-to-noise ratios at larger qubit counts.

As quantum computers advance, they are expected to contribute to other hypersonic chemistry and materials challenges, such as the development of lightweight, high-temperature materials and coatings. However, it is crucial to recognize that algorithms need to be capable of scaling to keep pace with the number of qubits available on devices. Without algorithmic breakthroughs that maintain computational fidelity at larger scales, the mere increase in qubit counts will not translate to practical simulation capabilities for complex systems. Longer term, quantum computers hold the potential to revolutionize fluid simulations, though this potential remains contingent on overcoming challenges in both hardware and algorithmic efficiency.

The study concludes by recommending quantum simulation of hypersonic atmospheric thermochemistry as an opportunity for investment. This application has the potential to improve the accuracy of hypersonic fluid simulations and the initial calculations are feasible on quantum computers available in 2025. In addition, quantum computing is a new technology for the aerospace industry, and in smaller orbital spaces, this application can serve as a quantum use case that is verifiable by classical computational methods. This is a necessary and important step for the aerospace industry to build confidence in quantum computing and opens the door to more advanced quantum use cases that will not be verifiable by classical computers.

An example of a classically-unverifiable, quantum use case is high entropy alloys (HEAs), and is a second application area for which further study is recommended. HEAs are typically defined as alloys that contain 5 or more elements in roughly equal proportion. These alloys are a remarkable class of materials that have demonstrated the highest strength-to-weight ratios and the highest yield strengths at high temperature (1200°C) of any known alloy[13,20]. However, these materials still face development challenges because they do not meet practical requirements, such as resistance to oxidation and corrosion. The HEA material space is vast, and experimental methods cannot efficiently explore it. Moreover, HEAs often contain transition metal elements, which are challenging for classical computers to simulate. As a result, this represents a potential high-impact opportunity that quantum computers may be able to address. However, today's quantum computers cannot yet simulate these materials. As a result, an investment is recommended to conduct diligence into this application to identify quantum computational requirements and estimate feasibility time frames.

We conclude this summary with several recommendations for quantum computing for the aerospace industry in general. Aerospace organizations should recognize that quantum computers have the potential to transform the industry and develop strategic plans that take into account the arrival of quantum error correction (QEC), a major advancement in the capabilities of quantum computers, expected in 2029.[21] Strategic plans should also identify key quantum opportunities and threats (this paper identifies some in the chemical and materials space) and address the severe shortage of talent in quantum computing. This requires establishing in-house expertise within both government and industry sectors to make informed decisions.

Developing proofs-of-concept is a crucial step that can serve as a vehicle for both evaluating quantum opportunities while also building quantum capabilities and cultivating talent. Early engagement is required, as the learning curve is steep. In IBM's experience, approximately 4 years are needed for organizations to master the technology and convert that mastery into applications. Organizations that start to build quantum capabilities in 2025 can intercept the arrival of QEC in 2029.

Collaborative, value-focused engagement from both industry and government is essential to ensure that the U.S. remains a global leader in commercializing this disruptive technology. Decision makers should be aware of an expected supply-demand mismatch due to sudden increase in demand for quantum computers. Once quantum computers are able to execute the first killer applications, demand is expected to suddenly increase. However, given their complexity and cost, the supply of quantum computers is likely to grow slowly. As a result, if access to quantum computers is not already secured, obtaining access may be challenging. Without access to quantum computers, talent will be challenging to attract. And without talent, intellectual property cannot be developed. The shortage may persist for years. As a result, Boston Consulting Group estimates that up to 90% of the benefits from quantum computers may be captured by early adopters.[25]

2 Introduction

Hypersonic flight, generally characterized as speeds greater than Mach 5, is a dual-use technology that has the potential to transform passenger travel, cargo delivery, and space flight. The high speeds of hypersonic flight can make possible a one-hour flight from New York to Tokyo. Currently, this flight takes 14 hours. Business travelers who typically plan intercontinental trips that require several days could consider flying to and from a meeting in a single day. The close connection of the world's cities by hypersonic flight opens the possibility of increased economic activity around the globe. The fast travel times of hypersonic flight also potentially enable the delivery of time-sensitive items, such as the transport of organs for transplants or critical parts for halted manufacturing lines. Finally, hypersonic craft may transform space access and the low earth orbit economy by enabling frequent and low-cost access to low earth orbit (LEO).

One characteristic that distinguishes hypersonic flight (generally greater than Mach 5) from supersonic flight (generally Mach 1-5) is the chemical activity of the atmospheric gases. At the extreme speeds, pressures, and temperatures of hypersonic flight, atmospheric gases such as O_2 and N_2, undergo chemical reactions. These reactions pose engineering challenges for developing hypersonic aircraft, including airframe design, materials development, and communications and sensor integration.

The empirical development of hypersonic platforms is time and cost intensive. Recreating Mach 5 conditions in a laboratory is challenging. For the experiments that can be conducted, experimental uncertainty is often on the order of 30% or more, depending on the models and methods used.[6] In addition, flight testing is costly and order of magnitude costs can be in the millions of dollars for a single flight test.

As a result, computational methods are expected to play an important role in the development of hypersonic platforms. However, hypersonic simulation performed on classical computers faces multiple challenges, such as speed and accuracy. These simulations are computationally intensive and can require days or weeks of computation time. At the extreme conditions of hypersonic flight, fluid flow can be highly nonlinear. As a result, small inaccuracies can grow to result in large overall inaccuracies.

Quantum computing is an emerging computation technology that *for some applications*, has shown to have the potential for polynomial or exponential reductions in the number of computational steps. As a result, there is great interest in the possibility of applying quantum algorithms to accelerate hypersonic development.

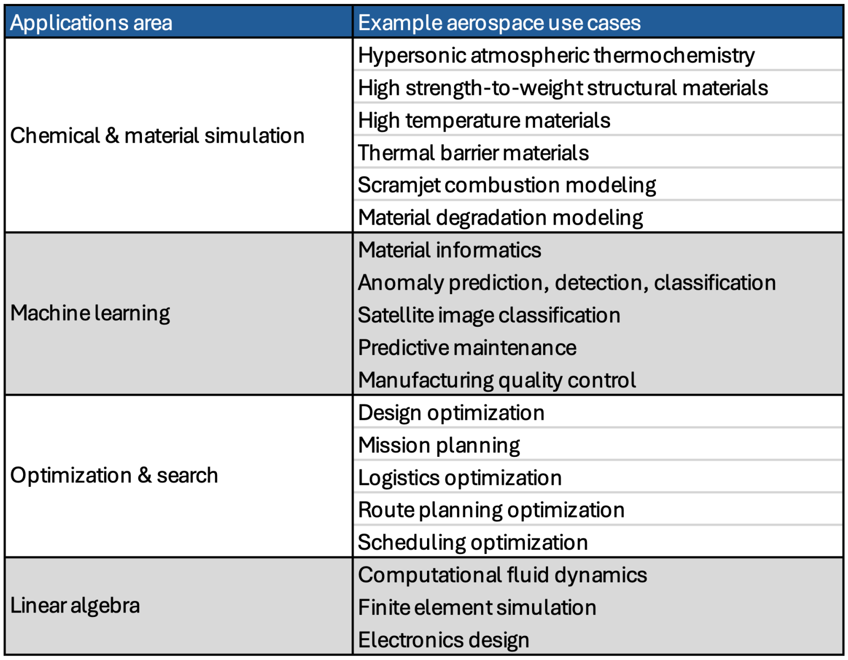

Applications area	Example aerospace use cases
Chemical & material simulation	Hypersonic atmospheric thermochemistry
	High strength-to-weight structural materials
	High temperature materials
	Thermal barrier materials
	Scramjet combustion modeling
	Material degradation modeling
Machine learning	Material informatics
	Anomaly prediction, detection, classification
	Satellite image classification
	Predictive maintenance
	Manufacturing quality control
Optimization & search	Design optimization
	Mission planning
	Logistics optimization
	Route planning optimization
	Scheduling optimization
Linear algebra	Computational fluid dynamics
	Finite element simulation
	Electronics design

Figure 1: Quantum computing major application areas and example aerospace use cases

Quantum computing has many possible applications. A list of the four most well-understood application areas with example aerospace use cases is in Figure 1. A white paper on quantum computing for aerospace that discusses some of these use cases in more depth can be found at the IBM Institute for Business Value.[8]

The current report focuses on the expected nearest-term application area for quantum computers, chemical and material simulation. Furthermore, this study identifies a near-term use case for quantum computing in hypersonic thermochemistry.

As mentioned before, perhaps the most challenging hypersonic atmospheric chemical reaction to simulate is the $N_2 + N_2 \rightarrow N_2 + 2N$ (N_4) reaction. Modeling this reaction accurately is important because N_2 is the most abundant gas in the atmosphere. State-of-the-art classical simulations have been conducted for the N_4 reaction.[30] However, the output from chemical simulations is the PES, which cannot be directly, empirically measured. Measurable quantities that result from the PES may be taken after a long chain of computations: the PES is inputted to molecular dynamics-type simulations to derive chemical reaction constants, which is inputted into hypersonic fluid flow simulations, which then may output measurable quantities, such as temperature, pressure, and fluid velocity.

Even after conducting the simulation chain, experimental measurements to verify the results may not be available. The database for experimental characterization of hypersonic phenomena is incomplete and measurements are difficult to obtain. Moreover, if the experimental value is available, and it does not match the computational value, the root cause of mismatch in the long chain of computations is unclear. However, it is often the case that up to the output of the molecular dynamics simulations, the PES is one of the largest sources of error[43].

Quantum simulation of the N_4 PES is therefore identified as an opportunity that has two potential benefits:

1. Quantum computers may serve as independent verification of the classical N_4 PES. This can increase confidence in hypersonic simulations that are difficult to verify empirically. Moreover, depending on the results, the quantum PES has the potential to compute a more accurate PES, which in turn may enable more accurate hypersonic fluid simulations.

2. The classical PES may serve as verification of the quantum PES to build confidence in quantum computers, a new technology for aerospace applications. This is an important step for quantum computations

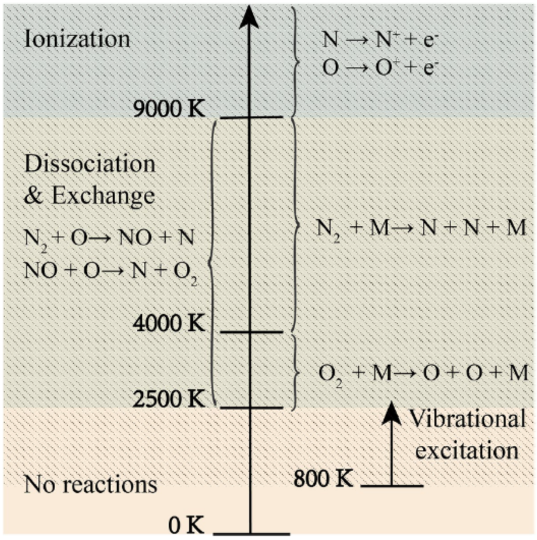

Figure 2: As airspeeds increase, the gas temperatures around the airframe increase, which causes chemical changes in the atmospheric gases starting at 800K.[47] Creative Commons license. http://creativecommons.org/licenses/by/4.0/

that are beyond verification by classical computations, such as simulations of advanced hypersonic materials, e.g., high-temperature and/or high strength-to-weight high entropy alloys.

This paper conducts diligence on the feasibility of quantum simulation of the N_4 system and other reactions in hypersonic atmospheric thermochemistry and concludes that computations with the STO-3G basis set[17] can be executed on quantum computers available today. Larger, more accurate basis sets are feasible in the next 1-3 years, depending on the basis set.

3 The chemistry and materials of hypersonic flight

There are a number of chemical and material challenges to hypersonic flight.

- Atmospheric gases undergo chemical reactions which changes the air composition which alters aerodynamic properties, such as lift and drag.
- Hypersonic structural materials need high strength-to-weight ratios.
- At the leading edges and within the engines, hypersonic structural materials must retain high strength at high temperatures.
- Hypersonic propulsion must combust fuels under extremely high flow conditions.
- Hydrogen gas, which is often used as fuel for hypersonic propulsion, embrittles materials and shortens their lifetimes.
- Thermal barrier materials are needed to enable hypersonic platforms to withstand temperatures into the tens of thousands of Kelvin. As a reference, the surface of the sun is 5,800K.
- The composition of the gases in the shock layer are not well understood. However, the shock layer is where the highest temperatures are generated and where reactive species such as atomic O and N are generated. These reactive species can erode the body of reusable hypersonic platforms, shortening their operating lifetimes, and negatively affecting performance.

Many aspects of the above chemistry and materials challenges are determined by quantum mechanical processes, such as:

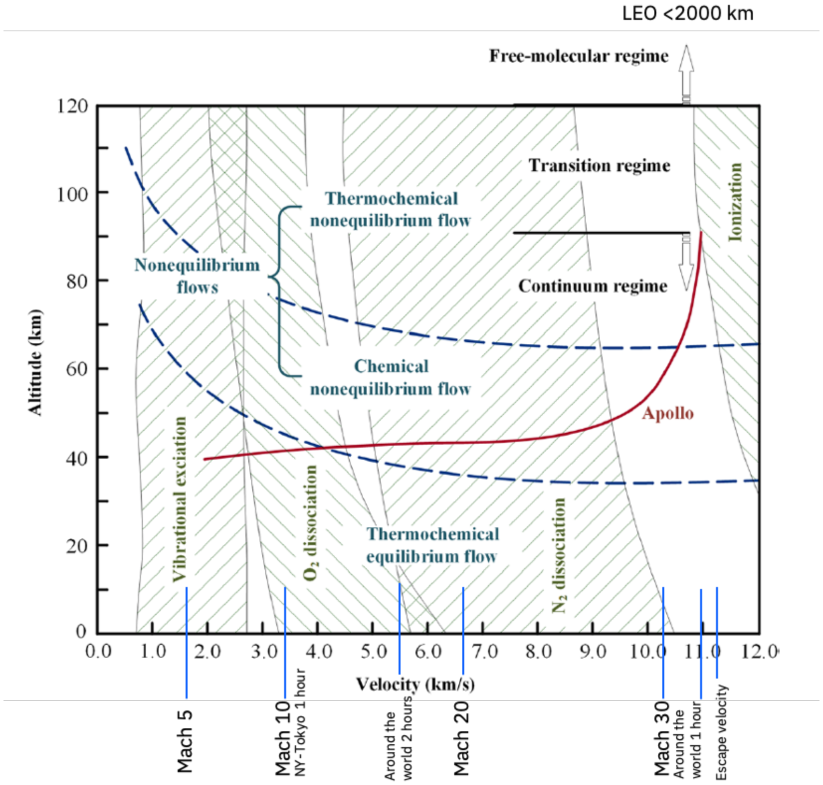

Figure 3: Regimes of flight velocity and altitude, illustrating the various atmospheric and thermodynamic conditions encountered by spacecraft during atmospheric entry.[47] Image modified from source. Creative Commons license. http://creativecommons.org/licenses/by/4.0/

- All of the reaction rates in the above examples, i.e., the dissociation of N_2 and O_2, the combustion of hydrogen, the hydrogen embrittlement of structural materials, the ablation of thermal barriers, etc., are determined by the electronic structures of the reactants, transition states, and products, which are, in turn, calculable from solving the Schrödinger equation, the quantum mechanical equivalent of Newton's Second Law, $\vec{F} = m\vec{a}$.
- A number of material properties, such as material elastic constants, coefficients of thermal expansion, reactivity with the environment, material ductility, material brittleness, temperature dependent material strengths, and many more, are calculable from solutions of the Schrödinger equation.

Many of these quantum phenomena are challenging to simulate with classical computers. However, the capabilities of quantum computers are a natural match to simulate quantum phenomena.

4 Classical computational challenges for chemical and material simulation

Classical computational chemistry has achieved significant success across many applications. However, fundamental limitations emerge when dealing with specific chemical phenomena, particularly those involving multi-reference chemistry.

Multi-reference chemistry arises when electrons occupy multiple orbital configurations, typically occurring when electron excitation energies approach or exceed orbital energy separations, electronic states are near-degenerate, or when chemical bonds are being formed or broken. This phenomenon is prominent in several aerospace-relevant chemical and materials systems, such as the breaking of N_2 bonds and excited states in atmospheric gases during hypersonic flight. Multi-reference situations also occur in transition metal materials (e.g., structural alloys) where closely spaced d orbitals allow multiple electron configurations.

In single-reference situations, the electrons occupy only one orbital configuration, enabling straightforward computation of electronic properties. In multi-reference situations, the number of possible electron configurations grows exponentially with system size (quantified by the number of orbitals and electrons in the system), which causes the number of computational steps to also grow exponentially. As a result, multi-reference chemical computations quickly become intractable, strongly restricting the size of simulable systems for classical computers.

For hypersonic atmospheric chemistry, additional challenges arise from strong electron correlation. O_2 double bonds and N_2 triple bonds can exhibit strong correlation effects during dissociation. Electron correlation manifests through both classical electrostatic interactions and quantum mechanical exchange effects. Density functional theory (DFT), despite being the most widely used computational chemistry method, often fails to accurately capture these strong correlation effects during bond dissociation processes. This inadequacy necessitates the use of more computationally intensive multi-reference methods that can properly describe electronic structure changes across varying internuclear distances.

Quantum computing offers a potential solution through: (1) Polynomial scaling with system size (versus exponential scaling for classical methods), (2) natural representation of superposition states, and (3) direct simulation of quantum mechanical effects.

Among the first hypersonic chemical applications feasible for quantum computing is simulation of chemical reactions involving N_2 and O_2. Their abundance in the atmosphere makes them the two most important species to model in atmospheric thermochemistry. Both molecules are small and therefore can be represented on near-term quantum computers. Yet their unique characteristics can make their chemical modeling challenging for classical methods.

Early quantum computing demonstrations of the disassociation of N_2 ground and excited states were published in 2024.[36,1] These methods may be extended to compute the PES of the N_4 reaction, as well as all other atmospheric reactions. Note that chemical accuracy was not demonstrated in these early results; however, chemical accuracy is believed to be achievable with larger active spaces and/or larger basis sets.

5 Hypersonic flight and atmospheric chemistry

Under hypersonic flight conditions, local air composition and hence local air chemistry determine local macroscopic air properties such as viscosity and thermal conductivity. These properties coupled with the local Mach number determine the local drag on a vehicle as well as the local surface temperature. Both have negative impacts on vehicle performance and structural response and integrity.[5] This environment is dominated by nitrogen and oxygen, which comprise approximately 99% of the atmosphere at sea level (78% N_2 and 21% O_2) with trace amounts of other gases such as Ar, CO_2, Ne, He, CH_4 making up the remaining 1%.

As aircraft travel through the atmosphere at high speeds, the forward kinetic energy of the aircraft results in high temperatures of the surrounding medium, particularly at the leading edges. These temperatures can exceed 2,000 K. As a reference, the temperature of the surface of the sun is 5,800 K. These high temperatures cause a series of chemical transformations. (see Figure 2)

Below 800 K, N_2 and O_2 behave as ideal gases in their ground states. At temperatures of 800 K and above, molecular rotational and vibrational modes become excited, marking the beginning of deviation from ideal gas behavior. This excitation significantly affects properties such as specific heats and dissociation rates, which impacts properties such as local viscosity and thermal conductivity.

The chemical environment becomes increasingly complex at higher temperatures. At 2500 K, O_2 begins to dissociate, initiating substantial changes in air composition. This dissociation process changes aerodynamic properties while also generating reactive atomic oxygen. As temperatures reach 4000 K, N_2 dissociation begins, further altering air composition and also generating reactive atomic nitrogen. The presence of both atomic oxygen and nitrogen accelerates the degradation of airframe materials.

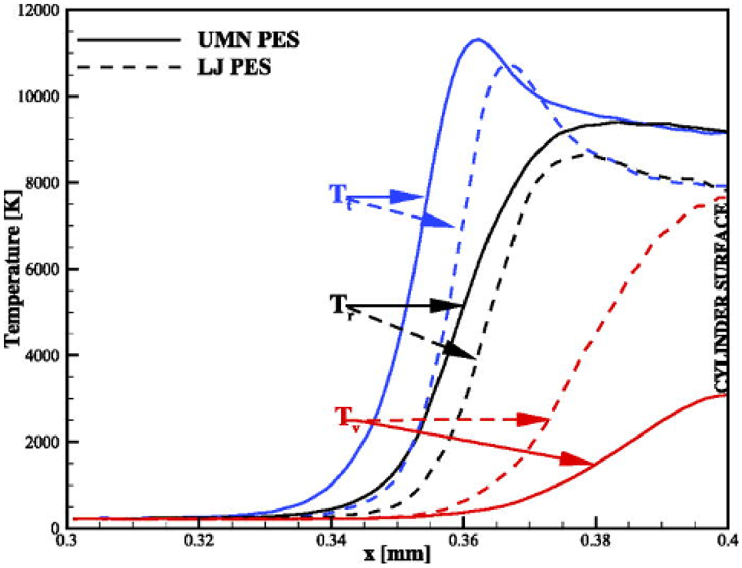

Figure 4: Comparison of temperature profiles predicted by two chemical models, the classically computed ab initio UMN PES and the empirically derived LJ PES, applied to the same hypersonic fluid simulation over a cylinder[15]. There are 3 lines for each model, describing the temperature profiles along the stagnation line for gas model's 3 temperatures, translational (T_t), rotational (T_r), and vibrational (T_v). The actual temperature that the surface experiences is the translational temperature. The temperature profiles at the cylinder surface differ by hundreds of degrees Kelvin for the translation and rotational lines, and thousand of degrees Kelvin for the vibrational line. The vibrational temperature is particularly significant since increased vibrational excitation increases dissociation rates, which increases changes in atmospheric composition. Maninder S. Grover and Paolo Valentini, Physics of Fluids, Vol. 33, 051704 (2021); used in accordance with the Creative Commons Attribution (CC BY) license (https://creativecommons.org/licenses/by/4.0/).

At temperatures of 9000 K and above, ionization processes begin to dominate the chemical environment. The liberation of free electrons leads to the formation of a plasma sheath around the vehicle, causing electromagnetic interference with sensors and antennas. This ionization layer can significantly impact communication and navigation systems, adding another layer of complexity to vehicle operation.

The cascade of chemical reactions and their interplay with aerodynamic forces presents a significant challenge for vehicle design and operation. Understanding and accurately modeling these chemical processes is crucial for predicting vehicle performance and developing protective measures against extreme conditions of hypersonic flight. The ability to accurately simulate these complex chemical interactions becomes particularly critical as the thermal environment transitions through different regimes, each presenting unique challenges for vehicle survivability and performance.

6 Hypersonic chemical model impacts on hypersonic fluid simulation

In addition to the dynamics of the structure, hypersonic simulation has two main interacting parts: the chemistry and the fluid flow. The accuracy of the chemical simulation impacts the accuracy of the fluid simulation. Hypersonic fluid simulation is strongly nonlinear and small inaccuracies can amplify to become large overall inaccuracies.

An example is a hypersonic fluid simulation of a cylinder using two different chemical models (Figure 4). One model is empirically derived (LJ PES) represented by dashed lines in the figure.[15] The other model is classically computed with state-of-the-art *ab initio* methods (UMN PES), represented by solid lines.[15]

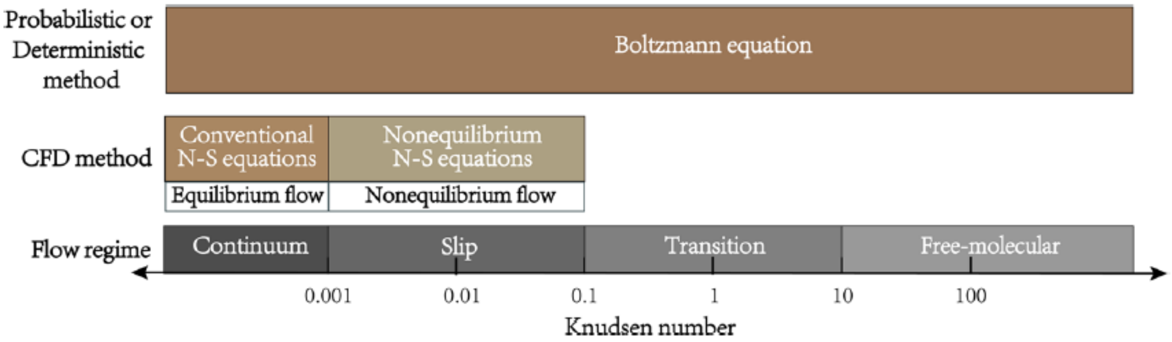

Figure 5: Continuum CFD is more computationally efficient, but is only applicable up to Knudsen numbers (K_n) of approximately 0.1. Particle based models, like the Boltzmann equation, are applicable across a wider range of K_n, but are more computationally expensive.[47] Creative Commons license. http://creativecommons.org/licenses/by/4.0/

Note that there are 3 temperatures in the figure, the translational temperature, T_t (blue), the rotational temperature, T_r (black), and the vibrational temperature, T_v (red). The temperature that a cylinder or airframe experiences is the translational temperature. Multiple temperatures are employed to preserve computationally efficient CFD methods while approximating excited-state distributions in the rotational and vibrational molecular degrees of freedom.

The temperature experienced by the cylinder, the translational temperature, T_t, differ by hundreds of degrees Kelvin between the two chemical models. This temperature difference is significant and directly impacts the heat flux experienced by the cylinder.[15]

The vibrational temperatures, T_v, differ by thousands of degrees at the cylinder surface between the two chemical models. Molecules in excited vibrational states have higher dissociation probabilities, which results in compositional differences of the air. Compositional differences, in turn, affect aerodynamic quantities, such as lift and drag, and material ablation rates, which impact airframe operational lifetimes.

Another example implication of atmospheric chemical changes for airframe design is predicting the transition location from laminar to turbulent flow. If the transition occurs at an important point, such as at a control surface, that part of the airframe must be moved or engineered to handle large heat loads or risk being damaged.[7] Composition and temperature differences both impact the transition location.

7 Hypersonic chemical and fluid simulation workflows

There are two types of fluid simulation models: continuum models based on the Navier–Stokes equations (“CFD method” in Figure 5) and particle models, e.g, DSMC “Probabilistic or Deterministic method” in Figure 5). Their applicable regimes are determined by the Knudsen number, K_n, the ratio of the mean free path to the characteristic flow length. Continuum computational fluid dynamics (CFD) is applicable for K_n <0.1. Continuum CFD is more computationally efficient and is preferred when applicable, particularly for large, complex fluid simulations, such as those for aircraft. Particle models are more accurate but more computationally intensive. They are applicable for all values of K_n, but tend to be used only when continuum CFD methods are not applicable.

Each model requires different outputs from the chemical models. In the continuum model, the interface between the chemical models and CFD is a set of chemical reaction constants. In the particle model, the interface is the chemical PES.

7.1 Chemical modeling in continuum fluid models

In continuum models, a common approach is to model the chemistry and fluid flow interaction through a coupled set of partial differential equations. There are three regimes: (1) Thermochemical equilibrium,

(2) thermal equilibrium, but chemical non-equilibrium (referred to as chemical non-equilibrium), and (3) thermochemical non-equilibrium.

In thermochemical equilibrium, the fluid flow is governed by the Navier–Stokes equations (Equations 1-3):[47]

$$\frac{\partial \rho}{\partial t} + \frac{\partial (\rho u_j)}{\partial x_j} = 0 \tag{1}$$

$$\frac{\partial}{\partial t}(\rho u_i) + \frac{\partial}{\partial x_j}\left(\rho u_i u_j + p\delta_{ij} - \tau_{ij}\right) = 0 \tag{2}$$

$$\frac{\partial E}{\partial t} + \frac{\partial}{\partial x_j}\left((E+p)u_j - \tau_{ij}u_i + q_j\right) = 0 \tag{3}$$

where ρ is the density, u is the velocity, δ_{ij} is the Kronecker delta, τ_{ij} is the shear stress tensor, p is the pressure, E is the total energy per unit volume, and q_j is the heat conduction vector.

Sufficient collisions are occurring between air molecules that equilibrium conditions can be assumed. Gas composition is dependent only on the temperature and pressure, which enables the uncoupling of the chemical reactions and flow equations.[47] Since the air is in chemical equilibrium, the chemistry can be described by the usual chemical reactions and reaction constants. Air properties can then be applied through lookup tables or fitted curves.

In chemical and thermochemical non-equilibrium , there are three gas models: (1) the 1-temperature, (2) 2-temperature, and (3) 3-temperature models. The three temperatures represent excited degrees of internal freedom for diatomic molecules, like N_2 and O_2. These degrees of freedom are the rotational, vibrational, and electronic. Note that these degrees of freedom are in addition to the usual translation degree of freedom for gas molecules.

For the case of 1-temperature model, the system is in thermal equilibrium (but not chemical equilibrium), and a single temperature, the translational temperature, may be used to characterize the system. In this case, the fluid Equations 1-3 are modified, as shown in Equations 4-6.[47]

$$\frac{\partial \rho_s}{\partial t} + \frac{\partial}{\partial x_j}(\rho_s u_j + J_{s,j}) = \dot{w}_s \tag{4}$$

$$\frac{\partial}{\partial t}(\rho u_i) + \frac{\partial}{\partial x_j}\left(\rho u_i u_j + p\delta_{ij} - \tau_{ij}\right) = 0 \tag{5}$$

$$\frac{\partial E_{ve}}{\partial t} + \frac{\partial}{\partial x_j}\left(E_{ve}u_j + q_{vej} + \sum_{s=1}^{ns} J_{s,j}h_{ve,s}\right) + p_e\frac{\partial u_j}{\partial x_j} = Q_{ve} \tag{6}$$

where $\dot{w}_s$ is the net source of the chemical species s due to chemical reactions.

For 2-temperature equilibrium, the rotational and translational modes are assumed to have the same temperature, and the vibrational and electronics modes are characterized by a different temperature to approximate their distribution among excited states. As a result, Equation 7 is added to Equations 4-6 for vibrational-electronic energy conservation:

$$\frac{\partial E_{ve}}{\partial t} + \frac{\partial}{\partial x_j}\left(E_{ve}u_j + q_{ve,j} + \sum_{s=1}^{n_s} J_{s,j}h_{v,s}\right) + p_e\frac{\partial u_j}{\partial x_j} = Q_{ve} \tag{7}$$

For 3-temperature equilibrium, the vibrational and electronic energy conservation are added separately (Equations 8 and 9). Note: Equation 7 is not used in the 3-temperature model.

$$\frac{\partial E_v}{\partial t} + \frac{\partial}{\partial x_j}\left(E_v u_j + q_{v_j} + \sum_{s=1}^{ns} J_{sj} h_{v_s}\right) = Q_v \tag{8}$$

$$\frac{\partial E_e}{\partial t} + \frac{\partial}{\partial x_j}\left[(E_e + p_e)u_j + q_{e_j} + \sum_{s} J_{s_j} h_{e,s}\right] - u_j \frac{\partial p_e}{\partial x_j} = Q_e \tag{9}$$

To compute the local air composition, transition rates between species are needed from the chemical models. The change in chemical composition of the air $\dot{w}_s$ in Equation 4 can be expressed in terms of the chemical reaction rates.[47] Note that molecules in different excited states are treated as different chemical species.

$$\dot{w}_s = M_s \sum_{r=1}^{NR} (\nu''_{s,r} - \nu'_{s,r}) \left[k_{f,r} \prod_{s=1}^{NS} \left(\frac{\rho_s}{M_s}\right)^{\nu'_{s,r}} - k_{b,r} \prod_{s=1}^{NS} \left(\frac{\rho_s}{M_s}\right)^{\nu''_{s,r}}\right] \tag{10}$$

where $\nu^{'}_{s,r}$, $\nu^{''}_{s,r}$ are the forward and backward stoichiometric coefficients of species s in the reaction r, k_f and k_b represent the forward and backward reaction rate coefficients, respectively, M_s is the molecular weight of species s.

For these regimes, several chemical models based on empirical data have been put forward. All of the chemical kinetic models have clear parameter tables in formula form, which can be used to calculate the reaction rate coefficients[47].

For these empirical chemical models, the uncertainty is high. For example, the rate constant for N_2 dissociation over the temperature range of interest (5000–10000 K) have an order of magnitude uncertainty across various databases.[37]

Owing to the uncertainty of empirical measurements, it is impractical to obtain accurate reaction rate coefficients experimentally. As a result, computational methods are the only method to estimate these coefficients.[47]

7.2 Chemical modeling in particle fluid models

In the particle picture, the interface between the chemical and particle simulations is the PES of each reaction. The PES is a multidimensional surface where potential energy is plotted as a function of nuclei position. The PES informs the particle model of the interaction forces between chemical species as a function of each nuclei position.

Computing the PES can be computationally intensive and is often source of the largest errors in particle fluid models.

7.3 Quantum computers in the hypersonic simulation workflow

To go from the quantum computation to hypersonic fluid simulation, the following workflow is adapted from papers by Truhlar et al.[30,3,15]

- The quantum computer calculates the PES.
- The PES serves as input to classical molecular dynamics simulations (or similar) to estimate chemical reaction coefficients.
- The chemical reaction coefficients are then employed by a classical continuum CFD solver.

For particle-based fluid modeling, the PES may be directly used.

For both particle-based fluid models and molecular dynamics simulations, it is often the case that the PES is one of the largest sources of error.[43] A number of approximations are required in the computation of the PES, particularly for multi-reference and strong correlation situations, such as with N_4 reaction. Quantum

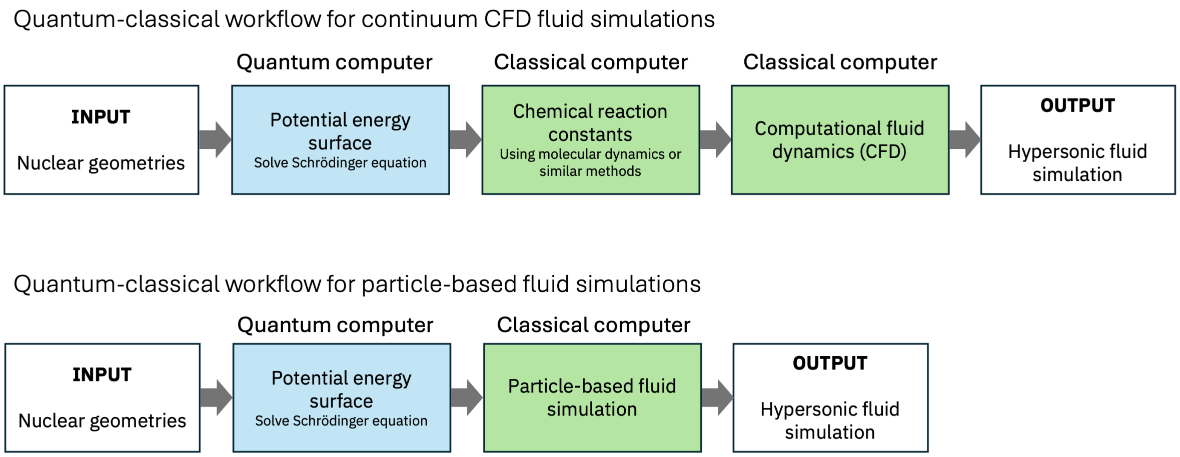

Figure 6: Quantum and classical computing workflows for hypersonic simulation for both contiuum and particle-based models. The workflow in Figure 7 is contained within quantum PES computation in this figure.

algorithms may model both effects with lower computational complexity, and therefore, potentially more accurately.

In both workflows, the quantum computer plays the same role, i.e., solving the Schrödinger equation to find the PES. The next section describes the activities within the quantum computations of the PES in more detail.

7.4 Classical PES development in hypersonic simulations

Classical electronic structure calculations for N_4 face significant challenges due to the system's complexity, with prior work limited to reduced four-dimensional PES models using rigid N_2 molecules and methods[4,18] like Configuration Interaction with Single and Double excitations (CISD) to Coupled Cluster with Single, Double, and perturbative Triple excitations (CCSD(T)).

The current state-of-the-art in this domain is the work by Truhlar's group[30], who developed a global *ab initio* ground-state PES for the N_4 system. This full-dimensional surface approach addresses the critical need to describe $N_2 - N_2$ interactions across a wide energy range, including dissociation pathways. Their methodology combines multi-reference electronic structure theory (with an active space containing 12 electrons and 12 orbitals) and advanced fitting techniques to balance computational feasibility and accuracy.

Their key results demonstrate the PES's capability to model high-energy phenomena. The PES reproduces Complete Active Space Second-Order Perturbation Theory (CASPT2) dissociation curves with an RMSE of 1.8 kcal/mol for energies below 100 kcal/mol, rising to 7.2 kcal/mol near the N_2 dissociation limit (≈ 228 kcal/mol). It captures critical features such as avoided crossings between electronic states, though the functional form inherently smooths cusps at state crossings–a limitation of single-surface adiabatic representations. Geometry optimizations of high-energy structures like tetrahedral N_4 align with theoretical benchmarks, but discrepancies emerge at very high energies ($E > 1000$ kcal/mol), where the fit prioritizes smooth gradients over strict adherence to *ab initio* cusps. By sampling $\approx 17{,}000$ nuclear geometries–spanning $N_2 - N_2$ and $N_3 - N$ configurations, variable bond lengths, and internal angles–the study overcomes limitations of earlier rigid models, providing a robust foundation for simulating hypersonic chemistry under extreme conditions.

8 SQD method and its application to N_4

We propose to use this comprehensive set of geometries by Truhlar et al.[30] as a framework for quantum computing calculations. At each coordinate, we can employ quantum computing algorithms such as Variational Quantum Eigensolver and SQD (both described below) to potentially obtain more accurate ground state energies for $N_2 - N_2$ systems. This approach leverages both the extensive geometric sampling of the classical PES and the potential advantages of quantum computing in electronic structure calculations.

The Variational Quantum Eigensolver (VQE)[32] has been a prominent hybrid quantum-classical algorithm designed to estimate the ground state energies of quantum systems, especially in quantum chemistry and condensed matter physics. VQE operates on the principle of variational optimization, where it seeks to minimize the expectation value of a Hamiltonian, which represents the energy of the system of interest E_0:

$$E_{\mathrm{VQE}} = \min_{\boldsymbol{\theta}} \langle \psi(\boldsymbol{\theta}) | H | \psi(\boldsymbol{\theta}) \rangle \ . \tag{11}$$

whereas the function E_{VQE} is evaluated on a quantum computer, and the parameters $\boldsymbol{\theta}$ are optimized on a classical computer. The quality of a VQE calculation depends on the ansatz and the convergence of the optimization procedure. For small systems, it's established that VQE can produce energies close to the exact diagonalization in the active space, known as the complete active space configuration interaction (CASCI)[35,29,12]. However, obtaining the lowest eigenvalues of Hamiltonian for complex systems necessitates the use of deep quantum circuits and extensive measurement protocols.

In 2024, IBM introduced Sample-based Quantum Diagonalization (SQD)[36], a new approach that integrates quantum computing with distributed classical computing to approximate eigenvalues for problem scales that exceed the capabilities of exact classical diagonalization. In SQD, the focus is on sampling from quantum states that approximate the eigenstates of the Hamiltonian, rather than optimizing a parameterized ansatz. These samples are used to construct a subspace in which the Hamiltonian can be classically diagonalized. Therefore, SQD can provide access to multiple eigenvalues, including excited states[1], since it samples across a range of states that can be tuned to cover different parts of the spectrum[40].

SQD offers distinct advantages over VQE, particularly for large-scale problems. By focusing on sampling rather than iterative optimization of a parameterized ansatz, SQD reduces the need for deep quantum circuits, making it more feasible on near-term quantum devices with limited coherence times. Furthermore, SQD can leverage HPC resources for efficient classical diagonalization of the subspace, allowing it to handle larger Hamiltonians. With high-qubit problems, VQE's iterative optimization becomes resource-intensive and challenging to scale.

8.1 SQD Theory

Sample-based Quantum Diagonalization is a variational approach for the search of eigenstates of many-body systems. The wavefunction's ansatz is based on the expansion of a general many-body state in a subset S of the basis of single-particle electronic configurations (Slater determinants) $\mathbf{x} \in \{0,1\}^{2N_{\mathrm{orb}}}$, where N_{orb} is the number of spatial orbitals. Using the Jordan-Wigner (JW) encoding scheme[22], each of the sampled bit strings corresponds to a configuration $\mathbf{x}$. The system size is characterized by the number of qubits required for the simulation, which scales as $2N_{\mathrm{orb}}$ for electronic structure problems. Provided that $|S|$ grows polynomially with the system size, the many-electron Hamiltonian can be projected and diagonalized in the subspace:

$$\hat{H}_S = \hat{P}_S \hat{H} \hat{P}_S \tag{12}$$

where the projector $\hat{P}_S$ is defined as $\hat{P}_S = \sum_{\mathbf{x} \in S} |\mathbf{x}\rangle\langle\mathbf{x}|$. The size and constituents of the subspace determine the accuracy of the wave function to represent the target eigenstate. Classical heuristics are available to identify the set of relevant configurations to include in S, collectively referred to as Selected Configuration Interaction (SCI) methods[11,41]. The original SQD paper demonstrated that a quantum circuit $|\Psi\rangle$ can also generate accurate statistical models capable of producing samples belonging to S[36].

The Localized Unitary Coupled-Cluster Jastrow (LUCJ) ansatz is a hardware-efficient unitary couple-cluster (UCC) ansatz used to produce the candidate ground states in SQD. The truncated version of LUCJ can be written as:

$$|\Psi\rangle = e^{\tilde{T}_{2\alpha} - \tilde{T}_{2\alpha}^{\dagger}} = \prod_{\mu} e^{-K_\mu} e^{iJ_\mu} e^{K_\mu} |\mathbf{x}_{RHF}\rangle \tag{13}$$

where $K_\mu = \sum_{pr} \kappa_{pr}^{\mu} \hat{a}_p^{\dagger} \hat{a}_r$ are the one-body operators, $J_\mu = \sum_{pr\sigma} J_{pr}^{\mu} \left[\hat{a}_p^{\dagger} \hat{a}_p\right] \left[\hat{a}_r^{\dagger} \hat{a}_r\right]$ are density-density operators restricted to spin-orbitals that are mapped onto adjacent qubits, and x_{RHF} is the bitstring representing the restricted Hartree-Fock (RHF) state in the JW mapping. The LUCJ circuits have moderate circuit depths due to exponentials of one-body operators, implementable in linear depth and a quadratic number of 2-qubit gates, and density-density operators, implementable in constant depth and a linear number of ZZ rotations. Using the JW encoding scheme, the LUCJ ansatz can be directly implemented on a quantum circuit without Trotter approximation, and has been demonstrated to obtain high accuracy while maintaining reduced circuit depths compared to the conventional qUCCSD ansatz.

The quantum hardware samples LUCJ circuits in the computational basis, generating a dictionary of bit strings that feeds into the SQD workflow. Since quantum noise tends to broaden the distribution of sampled configurations, SQD employs a self-consistent configuration recovery (SCCR) to probabilistically reconstruct noiseless configuration samples. This technique works by processing samples from the quantum processor and then projecting and diagonalizing a target Hamiltonian within the subspace defined by these samples. This approach makes SQD resilient against quantum noise corruption and capable of handling large Hamiltonians - including chemical systems with millions of interacting terms - that exceed the capabilities of exact diagonalization methods. Users provide quantum circuits that they believe effectively represent eigenstates (particularly ground states) of a target operator. The quality of these input samples directly affects performance: the more sparse the target eigenstate, the faster SQD converges as the number of samples increases.

The sufficient sampling size for SQD workflow depends on several factors, as demonstrated in the original SQD paper[36]. For the N_2 dissociation in cc-pVDZ basis, researchers employed 10^5 measurement outcomes with $K = 10$ batches, showing that increasing the subspace dimension d significantly improves both accuracy and physical consistency of potential energy surfaces. For more complex systems like the [4Fe-4S] cluster, much larger sampling was necessary. The study analyzed performance with up to $K = 100$ batches of configurations, revealing diminishing returns as batch numbers increased. Importantly, the sampling requirements scale with system complexity and sparsity of the target eigenstate, with more sparse representations requiring fewer samples to achieve convergence. The experiments suggest that optimal sampling involves balancing the subspace dimension d (affecting expressivity) with the number of configuration batches K (affecting statistical robustness), with both parameters needing to increase proportionally with system size and desired accuracy.

Robledo-Moreno et al.[36] leveraged up to 6,400 nodes of the Fugaku supercomputer to support a Heron superconducting quantum processor for three advanced chemistry experiments: the bond-breaking of N_2 utilizing 58 qubits and 5,204 quantum gates, and active space simulations on eigenstates of two [Fe-S] clusters - [2Fe–2S] dimer utilizing 45 qubits and 3,170 quantum gates, [4Fe–4S] cage utilizing 77 qubits and 10,570 quantum gates. This was a key development in quantum computing, which demonstrates that accurate energy approximations do not require exact ground state distribution reconstruction, and sampling from noisy ground state configurations and using SCCR allows for accurate solutions.

Recent extensions of SQD have enabled electronic structure calculations for supramolecular systems[23], open-shell systems[27], and excited states[1] using quantum computers. The current implementation of the SQD method is part of the `qiskit-addon-sqd` Python package. The classical projection and diagonalization can be obtained with the Davidson method implemented in the library PySCF[42] on a single computing node, or DICE[19,41] for distributed computing on multiple nodes.

The application of SQD to the calculations of PES of molecules and reactions relevant to hypersonic chemistry problems currently faces important limitations that define the scope of its practical use. At present, SQD implementations are restricted to electronic structure calculations, requiring nuclear coordinates to be supplied from classical calculations such as the PES coordinate sets from Truhlar's group[30]. In this workflow, SQD serves to refine the ground state energy at each nuclear configuration point, providing high-accuracy electronic energies that can be used to construct PES.

This limitation stems from the fundamental challenge of simultaneously treating electronic and nuclear degrees of freedom in quantum chemistry calculations. While SQD has demonstrated notable capabilities in handling electronic structure problems, as evidenced by successful applications to complex systems like [Fe-S] clusters and bond dissociation in N_2, the method currently relies on the Born-Oppenheimer approximation and treats nuclear positions as classical parameters rather than quantum degrees of freedom.

Looking toward future hypersonic applications, a key goal is to extend SQD methodology to address vi-

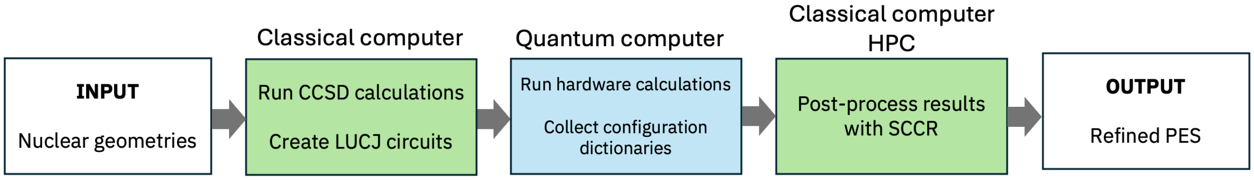

Figure 7: Schematic representation of the SQD workflow. Note that these steps are within the quantum PES box in Figure 6.

bronic problems directly. This would enable the generation of complete PES without dependence on classical methods for nuclear coordinate sampling. Such an advancement would be extremely valuable for hypersonic applications, where accurate representation of coupled electronic-nuclear dynamics is crucial for understanding hypersonic phenomena, including non-adiabatic transitions between electronic states during molecular dissociation, vibrational energy redistribution in high-temperature environments, quantum effects in reaction rate calculations under extreme conditions, and anharmonic coupling between vibrational modes.

The extension of SQD to vibronic problems would require significant theoretical developments. Modified sampling strategies are needed to efficiently explore both electronic and nuclear configuration spaces. The quantum computing portion requires enhanced ansatz designs that can represent coupled electronic-nuclear wavefunctions. Last but not least, classical post-processing methods need to be adapted for handling the increased dimensionality of the problem.

8.2 Hybrid HPC-quantum architecture

The implementation of a hybrid HPC-quantum architecture for hypersonic simulations combines quantum computing with classical fluid modeling capabilities. The workflow begins with the SQD method running on quantum hardware supported by distributed classical computing resources to refine the PES calculations. For each of the input nuclear coordinates (such as the data set by Truhlar's group[30]), SQD provides high-accuracy electronic energies that are collected and processed using classical HPC systems to construct the complete PES. Then this refined PES data then feeds into either pathway: for continuum CFD, it drives molecular dynamics simulations on classical computers to compute chemical reaction coefficients for the CFD solver; for the particle-based method, it directly informs the intermolecular force calculations in the particle simulation codes. This architecture leverages quantum computing's advantage in electronic structure calculations while utilizing classical HPC's proven capabilities in fluid dynamics simulations.

9 Feasibility assessment

The resource assessment for the SQD algorithm is mainly based on the hardware sampling requirements of the LUCJ ansatz. In this assessment, one layer of the ansatz is used. Quantum circuits were constructed using the `ffsim`[45] software library, which enables efficient simulation of fermionic quantum circuits by exploiting symmetries and specialized algorithms. When qubitized using the Jordan-Wigner transformation, the N_4 system requires between 32 to 176 qubits, depending on the basis set chosen.

The choice of basis set is crucial in the SQD workflow as it directly impacts the accuracy of the Hartree-Fock reference state used in the LUCJ circuit initialization. Larger basis sets provide a more complete spatial representation of molecular orbitals, enabling better description of electron correlation effects and more accurate energetics in the final SQD calculations. However, this improved accuracy comes with increased computational cost.

For an equivalent active space selection–such as the (12e, 12o) active space used in Truhlar's work[30]–we do not expect SQD with perturbative corrections (SQD+PT2) to improve upon CASPT2 results. This is because CASPT2 already performs a full configuration interaction (CI) calculation within the active space, representing the theoretical accuracy limit for that active space. The true advantage of SQD lies not in surpassing CASPT2 for identical active spaces, but rather in its potential to handle substantially larger active spaces that would be computationally prohibitive for classical CASPT2 approaches. Therefore, the resource estimate shows the requirements needed for performing SQD for the full system, only subtracting the frozen core. This is particularly important for accurately describing the N_4 reaction, especially in transition states and dissociation regions where multi-reference character becomes dominant.

From a computational perspective, the dimensionality of the required subspace to accurately characterize the ground state grows exponentially with system size. This growth is further exacerbated by the use of larger basis sets, which increase the number of orbitals and the corresponding number of qubits required to represent the system. For N_4, even with the minimal STO-3G basis set, the system requires 32 qubits and over 5,000 quantum gates. With larger basis sets like aug-cc-pVDZ, the requirements increase dramatically to 176 qubits and over 130,000 quantum gates. Applying SQD to systems exceeding 52 orbitals (104 qubits) may demand substantial classical resources, including petabyte-scale RAM and thousands of multi-core CPU nodes.

The feasibility of executing the LUCJ ansatz for the dissociation curve of N_4 on quantum hardware depends on the resource requirements outlined in Table 1 and the anticipated advances in quantum computing. Current hardware struggles to execute circuits of significant depth due to limitations in gate fidelity and qubit coherence, but these challenges are fundamentally algorithmic as well as hardware-related. While IBM's quantum roadmap anticipates substantial hardware improvements—with the ability to run circuits with up to 10,000 gates by 2027, 15,000 gates by 2028, and 100 million gates in 2029 (see IBM roadmap in Figure 8)—these advancements alone will be insufficient. The practical ability to model complex reactions like N_4 will depend critically on corresponding algorithmic advances that maintain sufficient signal-to-noise ratios at larger qubit counts. Even with minimal STO-3G basis set calculations (requiring 32 qubits and approximately 5,300 total gates), which may appear manageable on existing quantum devices, algorithmic limitations effectively restrict practical computations to approximately 70 qubits due to rapidly decreasing signal-to-noise ratios. For larger basis sets such as aug-cc-pVDZ, both hardware and algorithmic breakthroughs will be necessary to achieve meaningful results. Therefore, while hardware improvements are following a clear roadmap, the timeline for practical N_4 simulations remains dependent on parallel advances in error mitigation techniques and algorithmic improvements.

Basis set	**# orbitals**	**# qubits**	**# 1-q gates**	**# 2-q gates**	**Depth**
STO-3G	16	32	4538	788	306
cc-pVDZ	52	104	42581	7214	882
aug-cc-pVDZ	88	176	111728	18824	1458

Table 1: Estimated resources for electronic structure calculations on the PES of the N_4 system using the Jordan-Wigner mapping. Note that the number of orbitals is without the frozen core and the number of qubits does not include the ancilla qubits required on actual hardware.

10 Quantum computers for other hypersonic chemistry and materials use cases

As quantum computers advance, it is expected that they will contribute to other hypersonic chemistry and materials challenges. A list of example use cases includes:

- High strength-to-weight structural materials[28]
- High temperature structural materials[20]
- Thermal barrier materials[33]
- Material degradation and lifetime estimation[33]
- Hypersonic propulsion combustion modeling[24]
- Hydrogen embrittlement from H_2 fuel[10]

High entropy alloys are an interesting family of materials to explore for aerospace. These alloys are characterized by having nearly equal amounts of at least 5 elements, in contrast to most alloys, which are typically dominated by 1 or 2 elements. HEAs have demonstrated remarkable properties; for example, the highest known strength-to-weight ratio for any metal is a high entropy alloy, $Al_{20}Li_{20}Mg_{10}Sc_{20}Ti_{30}$[28]. Another example is the highest yield strength at 1200°C for alloys was demonstrated by a HEA, $MoNbTaVW$[20]. For a comparative overview of yield strength across conventional alloys and refractory HEAs, see Figure 1 in the study by Huang and Liaw[20].

However, HEAs still face a number of developmental hurdles. For example, while HEAs may exhibit remarkable properties in one important aspect, such as strength-to-weight ratio, they may have deficiencies in other aspects, such as they may not be sufficiently ductile, or they may not exhibit sufficient resistance to oxidation or corrosion, or they may not be stable over time.

A HEA that has the right combination of properties may exist. But, the number of alloys possible with the combination of five or more elements results in a vast materials space that is too enormous to explore experimentally. Only computational methods may efficiently explore this space. But, one challenge for classical computational methods is that many HEAs contain transition metal elements. For example, both the highest strength-to-weight ratio HEA and the highest yield strength at 1200°C HEA contain transition metal elements. Transition metal materials are often multi-reference, and as a result, classical simulation of these materials will be challenged. Moreover, reaction rates such as for oxidation and corrosion processes can be challenging to model with classical methods.[2] Quantum computers, on the other hand, have already simulated a transition metal molecule in 2024.[36] Transition metal materials have not been demonstrated yet, but are expected to be possible with more capable quantum computers. This opens the door to computational exploration of the HEA space and the potential identification of HEAs that have the required set of properties for high-performance aerospace applications.

Estimations for feasibility time frames to simulate HEAs is beyond the scope of this document. However, it is known that the unit cell for HEAs is large, on the order of 100 atoms, implying large active spaces that are not feasible on currently available quantum computers. But quantum computers that can handle thousands of orbitals are on the IBM Quantum Roadmap. And embedding and other techniques may be able to reduce the requirements on quantum computers.

HEAs represent a potential high-impact area of application for quantum computers. This is an application where investment should be considered in order to conduct deeper diligence on the computational requirements and to estimate feasibility time frames.

11 Quantum computers for fluid simulation

Simulating fluid flows is typically the largest computational load for the aerospace industry. As a result, there is great interest in applying quantum computers to this problem. Currently, simulating fluid flows is considered a longer-term application for quantum computers and is an active area of research.

The most computationally intensive part of CFD is the matrix inversion. The Harrow–Hassidim–Lloyd (HHL) family of quantum algorithms can exponentially accelerate this part of the computation.[16] This remarkable result opens the possibility that simulations of arbitrary size and resolution may be executed on quantum computers.

For example, possible exponential speedup has been identified for weakly compressible fluids at arbitrary Reynolds numbers at speeds much less than Mach 1.[26] The potential applications for this regime is enormous, including maritime craft design, automotive design, oil and gas flow, cardiac hemodynamic simulations, and many more.

However, the aerospace industry is typically interested in compressible fluids at speeds that are at a significant fraction of or greater than Mach 1. There are several identified challenges to applying quantum computation to aerospace fluid flow simulations, that reserve this quantum application as a longer-term quantum application:

11.1 Quantum circuit width and depth requirements

Penuel et al. published resource estimates for a sphere in a low speed, weakly compressible fluid at a Reynolds number of 500. They estimate that the required number of logical qubits is on the order of 10^5 and the number of T gates is on the order of 10^{23}.[31] To put this in perspective, the IBM Quantum roadmap plans for quantum computers with 2000 logical qubits executing 10^9 2-qubit gates (one T-gate can approximated as one 2-qubit gate) in 2033. Given the current status of quantum hardware and algorithms, fluid simulation seems quite far away.

However, the authors of the paper[31] point out that these estimates should be considered a weak upper limit as their estimate is a reflection of the current immaturity of quantum algorithms. Other areas of quantum application, such as cryptography[34] and chemical simulation,[36] have seen algorithmic advancements that result in orders of magnitude reductions in the required quantum computational resources. In both cases, the improvements came from combining quantum computers with high performance classical computers, which has yet to be applied to quantum algorithms for CFD.

11.2 Nonlinearity

Part of the reason that so many qubits and 2-qubit gates are required is because the Navier–Stokes equations are nonlinear. In the Penuel et al. paper, they handle the nonlinearity with Carleman linearization that yields an infinite set of differential equations, which are then truncated. This results in large increases in both the number of qubits and 2-qubit gates, particularly for high-resolution simulations, which are needed for modeling phenomena such as turbulence.[31] However, there are other ways to handle the nonlinearity, including hybrid methods,[44] mean-field methods,[44] transforming the Navier–Stokes equations to the Schrödinger equation via the Madelung transform,[38] and many others. Algorithmic advancements in handling the nonlinearity may have a large impact on both qubit count and 2-qubit gate count.

11.3 Input and output interfaces

Another challenge for applying quantum computers to fluid simulation is that the interfaces between classical and quantum computers are currently low bandwidth. To transfer a large, detailed model to and from a quantum computer may take so many operations that it can negate even exponential speedups possibly attainable by a quantum computer.

In addition, after the quantum computer has completed its computation, the solution vector in the quantum computer is stored as a superposition over multiple qubits. When a measurement for readout is taken, the superposition collapses and only 1 scalar value may be outputted. The entire solution vector may be recovered by running the simulations multiple times, but this negates any speedup from a quantum algorithm.

Approaches to the classical-to-quantum input problem are being approached at several different layers of the quantum computing stack. For example, at the hardware level, a hypothetical device called QRAM could efficiently load complex data into a quantum computer.[14] At the algorithmic level, methods to load matrices and vectors with certain structures have been identified. For example, efficient methods to load Toeplitz matrices is known.[46]

At the workflow level, innovation in applying quantum algorithms to CFD is yielding ways to solve both the input and output problems. This requires quantum algorithms to be applied to CFD differently from classical equivalent algorithms. For example, the input/output problems discussed above use a quantum computer in the exact same way one would use a classical computer. A potentially more effective way to use a quantum computer may be *not* to ask *what is the fluid velocity at every point in space?*, as is done with classical methods. Instead, a more fruitful question may be to ask quantum computers *what is the best design?* This was demonstrated in a paper by Sato et al.[39] Counterintuitively, they show it can be easier to load into a quantum computer all possible designs of a topological optimization design space than it is to load a single design. The quantum computer then simulates all possible designs simultaneously and outputs a single scalar value that identifies the best design. Once the best design is identified, it may then be simulated on classical computers to obtain the fluid velocity at every point in space, or whatever quantity is simulated.

The potential impact of exponential acceleration of fluid flow simulation is expected to be revolutionary for the aerospace industry. However, the question of whether and/or when advances in quantum computation will address the above fluid simulation challenges is unpredictable. As a result, the aerospace industry is advised to develop capabilities to monitor advancements and experiment with quantum algorithms to identify workflows that can leverage the quantum algorithms' unique capabilities and requirements.

12 Quantum computing status and trends

12.1 Quantum hardware

Quantum computing hardware is making remarkable progress. Looking at the IBM Quantum roadmap in Figure 8, two trends emerge. First, the qubit count is increasing. The first quantum computer was made publicly available on the cloud in 2016. That quantum computer had 5 qubits. In 2023, a quantum computer with over 1100 qubits was in operation. Looking forward, a quantum computer with 200 logical qubits (physical qubit count is on the order of magnitude of 10,000 qubits) is expected in 2029. And a quantum computer with 2000 logical qubits (physical qubit count is on the order of 100,000 qubits) is expected in 2033.

The second trend is in the number of 2-qubit operations that may be executed. In 2025, 5000 2-qubit gates may be executed. This is expected to triple by 2028 to 15,000 gates. In 2029, the number of 2-qubit gates operations makes a jump to 100 million gates in 2028 and 1 billion gates in 2033.

The jump in gate count in 2029 is due to the arrival of quantum error correction (QEC). QEC is a method to combine multiple, noisy, short-lived physical qubits, into ideal, long-lived logical qubits.

12.2 Quantum algorithms

The development of quantum algorithms is currently experiencing several trends. In the first wave of quantum algorithms, circa pre-2014, the primary question was: Are there calculations that quantum computers can do that offer some benefit over classical algorithms? The outcome was that several algorithms were identified, including Shor's algorithms, Grover's algorithm, HHL, Hamiltonian simulation, and many more.

In the current wave of quantum algorithms, the question has shifted to: Are there useful quantum algorithms that can be executed on near-term quantum hardware?

In the first wave, the quantum algorithms identified were often embodied as a single large quantum circuit. This facilitated analysis of these algorithms. In the second wave, the algorithms are often combined quantum and classical computations that enable execution with fewer quantum resources. An example are the variational algorithms, such as VQE. A more recent example uses multiple quantum circuits to drastically reduce the hardware requirements for Shor's algorithm by orders of magnitude.[34] Yet another example is sampling based methods, such as SQD.[36]

In contrast to the quantum hardware, advances in algorithms are harder to predict. There are aspects to the hardware that can make predictable progress to the point that technology roadmaps may be published. Algorithms, on the other hand, have a punctuated pattern of improvement with both the magnitude and timings of the improvements occurring unpredictably.

Given the impact of algorithmic improvements and their unpredictable nature, the quantum algorithm literature needs to be monitored. However, this requires the capability to understand the literature and the ability to interpret its impact for the aerospace industry and individual aerospace organizations.

13 Conclusion and Recommendations

Hypersonic platforms represent a transformative opportunity for passenger transport, cargo delivery, and space access. However, their development faces significant challenges due to extreme flight conditions. Traditional empirical approaches are both costly and time-intensive, often yielding results with large uncertainties. This has led to an increasing reliance on computational methods to advance hypersonic development.

One of the key challenges in hypersonic aircraft development involves understanding and simulating quantum mechanical phenomena in materials and chemical systems. While these simulations prove challenging for classical computers, they align naturally with the capabilities of quantum computers.

The 2029 arrival of QEC is expected to widen the application space for quantum computers. However, the first applications are possible before QEC. An example is the N_4 thermochemistry described in this document.

Accurate hypersonic atmospheric thermochemical models are needed for hypersonic platform development, but are challenging for classical computers to simulate due to multi-reference and strong electron correlation effects. The N_4 reaction is a key reaction for hypersonics, and among the most challenging reactions for which to calculate a potential energy surface. The PES is often one of the largest sources of error for molecular and other particle based simulations, which are required for both continuum and particle hypersonic fluid simulations.

SQD is a recent advancement in quantum computing that enables solving the Schrödinger equation for multi-reference and strongly correlated chemical and materials systems. This paper examines the feasibility of applying SQD to the N_4 system and concludes that initial calculations are feasible on quantum computers available in 2025.

Quantum computation of the N_4 reaction PES can serve several purposes:

- Quantum verification of the classical PES
- Classical verification of the quantum PES, an important and necessary step to build confidence towards acceptance of quantum calculations by aerospace industry. This confidence will be needed for more advanced quantum computing aerospace use cases that will not be verifiable by classical computers.
- Potential increased accuracy of the PES, dependent upon the results.

This article has focused on quantum computing for chemical simulation. However, the application space for quantum computers is much wider. While chemical and material simulations are likely the nearest term application area for quantum computers, several other areas have been identified as near-term, including machine learning and optimization. CFD is a potential application that is likely further into the future and is an active area of research.

This article concludes with several recommended actions for aerospace industry:

- Invest in capabilities to conduct quantum simulation of hypersonic atmospheric thermochemistry. This is an opportunity whose initial calculations are feasible on quantum computers in 2025 that has multiple potential benefits. People, time, and access to quantum computers will be needed to conduct this calculation.
- Invest in diligence on quantum computation for high entropy alloys. This is a potential high-impact use case that can be uniquely addressed by quantum computers, however it is not yet feasible. A study to conduct diligence into this use case and estimate feasibility time frames is recommended.
- Aerospace organizations should develop strategic plans for quantum computing that address:
  - The 2029 arrival of quantum error correction, an expected major advance in the capabilities of quantum computers.
  - The expected supply-demand mismatch due to the sudden increase in demand when the first killer applications are executing on quantum computers. Organizations that have not secured access after this time may not be able to access quantum computers for years. Without access, organizations cannot attract talent and develop intellectual property. As a result, BCG estimates that up to 90% of the value created by quantum computers will be captured by early adopters.
  - Identification of key quantum opportunities and threats and their feasibility time frames.
  - The scarcity of quantum computing talent. Organizations are unlikely to be able to hire quantum computing teams. As a result, talent should be developed in-house.

  - The steep learning curve. In IBM's experience, organizations need approximately four years to independently develop applications. Two years are needed to master the technology and two years are needed to convert that mastery into applications.

- Because of the steep learning curve, early engagement is needed. For the aerospace industry value stream including the industry and government sectors, start the process to establish quantum capabilities in 2025 to intercept quantum error correction in 2029.
- Developing proofs-of-concept is a crucial activity that enables the evaluation of quantum opportunities while also developing quantum talent.
- Finally, join a quantum ecosystem. No one can do this alone. Quantum ecosystems can provide access to quantum hardware, software development platforms, and knowledge sharing. Consider ecosystems with open-source software development platforms that enable leveraging a broad and deep code base.

14 Acknowledgment

This material is based on research sponsored by Air Force Research Laboratory under agreement number FA8650-22-2-5720. The U.S. Government is authorized to reproduce and distribute reprints for Governmental purposes notwithstanding any copyright notation thereon.

15 Disclaimer

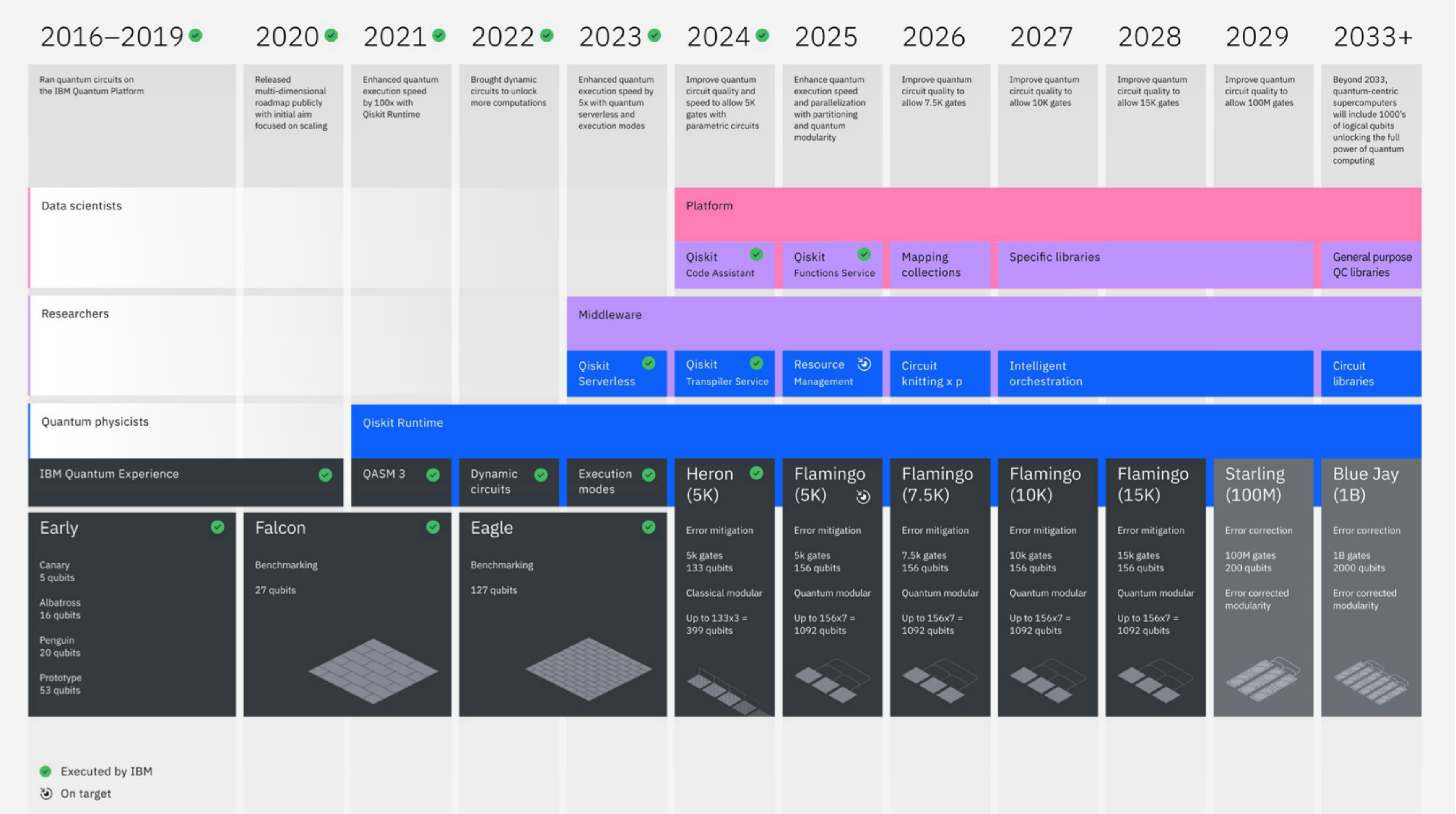

	2016–2019 ✓	2020 ✓	2021 ✓	2022 ✓	2023 ✓	2024 ✓	2025	2026	2027	2028	2029	2033+
	Ran quantum circuits on the IBM Quantum Platform	Released multi-dimensional roadmap publicly with initial aim focused on scaling	Enhanced quantum execution speed by 100x with Qiskit Runtime	Brought dynamic circuits to unlock more computations	Enhanced quantum execution speed by 5x with quantum serverless and execution modes	Improve quantum circuit quality and speed to allow 5K gates with parametric circuits	Enhance quantum execution speed and parallelization with partitioning and quantum modularity	Improve quantum circuit quality to allow 7.5K gates	Improve quantum circuit quality to allow 10K gates	Improve quantum circuit quality to allow 15K gates	Improve quantum circuit quality to allow 100M gates	Beyond 2033, quantum-centric supercomputers will include 1000's of logical qubits unlocking the full power of quantum computing
Data scientists						Platform						
						Qiskit Code Assistant ✓	Qiskit Functions Service ✓	Mapping collections	Specific libraries			General purpose QC libraries
Researchers					Middleware							
					Qiskit Serverless ✓	Qiskit Transpiler Service ✓	Resource Management ◷	Circuit knitting x p	Intelligent orchestration			Circuit libraries
Quantum physicists			Qiskit Runtime									
	IBM Quantum Experience ✓		QASM 3 ✓	Dynamic circuits ✓	Execution modes ✓	Heron (5K) ✓ Error mitigation 5k gates 133 qubits Classical modular Up to 133x3 = 399 qubits	Flamingo (5K) ◷ Error mitigation 5k gates 156 qubits Quantum modular Up to 156x7 = 1092 qubits	Flamingo (7.5K) Error mitigation 7.5k gates 156 qubits Quantum modular Up to 156x7 = 1092 qubits	Flamingo (10K) Error mitigation 10k gates 156 qubits Quantum modular Up to 156x7 = 1092 qubits	Flamingo (15K) Error mitigation 15k gates 156 qubits Quantum modular Up to 156x7 = 1092 qubits	Starling (100M) Error correction 100M gates 200 qubits Error corrected modularity	Blue Jay (1B) Error correction 1B gates 2000 qubits Error corrected modularity
	Early ✓ Canary 5 qubits Albatross 16 qubits Penguin 20 qubits Prototype 53 qubits	Falcon ✓ Benchmarking 27 qubits		Eagle ✓ Benchmarking 127 qubits								

✓ Executed by IBM

◷ On target

Figure 8: IBM Quantum roadmap.[21]

References

[1] Stefano Barison, Javier Robledo Moreno, and Mario Motta. “Quantum-centric computation of molecular excited states with extended sample-based quantum diagonalization”. In: *ArXiv Preprint arXiv:2411.00468* (2024).

[2] Bela Bauer et al. “Quantum algorithms for quantum chemistry and quantum materials science”. In: *Chem. Rev.* 120.22 (2020), pp. 12685–12717.

[3] Jason D Bender et al. “An improved potential energy surface and multi-temperature quasiclassical trajectory calculations of $N_2 + N_2$ dissociation reactions”. In: *J. Chem. Phys.* 143.5 (2015).

[4] Hans-Joachim Böhm and Reinhart Ahlrichs. “The $N_2 - N_2$ interaction: A theoretical investigation”. In: *Mol. Phys.* 55.5 (1985), pp. 1159–1169.

[5] Michael Brown. *Interview on hypersonic thermochemistry.* Personal communication on 02/06/2025.

[6] Ross S Chaudhry. “Modeling and analysis of chemical kinetics for hypersonic flows in air”. PhD thesis. University of Minnesota, 2018.

[7] Vincent Aiello Daniel Millman. *Hypersonics.* Fighter Pilot Podcast. Apple Podcasts, Apr. 2023. URL: `https://podcasts.apple.com/us/podcast/fighter-pilot-podcast/id1330534712`.

[8] Bob Dirgo, Charles Chung, and Thomas Ward. *Exploring quantum use cases for the aerospace industry.* Tech. rep. IBM Institute for Business Value, 2024. URL: `https://www.ibm.com/thought-leadership/institute-business-value/en-us/report/quantum-aerospace`.

[9] Thom H Dunning Jr. “Gaussian basis sets for use in correlated molecular calculations. I. The atoms boron through neon and hydrogen”. In: *J. Chem. Phys.* 90.2 (1989), pp. 1007–1023.

[10] Suhas Eswarappa Prameela et al. “Materials for extreme environments”. In: *Nat. Rev. Mater.* 8.2 (2023), pp. 81–88.

[11] Francesco A Evangelista. “Adaptive multiconfigurational wave functions”. In: *J. Chem. Phys.* 140.12 (2014).

[12] Qi Gao et al. “Computational investigations of the lithium superoxide dimer rearrangement on noisy quantum devices”. In: *J. Phys. Chem. A* 125.9 (2021), pp. 1827–1836.

[13] Easo P George, Dierk Raabe, and Robert O Ritchie. “High-entropy alloys”. In: *Nat. Rev. Mater.* 4.8 (2019), pp. 515–534.

[14] Vittorio Giovannetti, Seth Lloyd, and Lorenzo Maccone. “Quantum random access memory”. In: *Phys. Rev. Lett.* 100.16 (2008), p. 160501.

[15] Maninder S Grover and Paolo Valentini. “Ab initio simulation of hypersonic flows past a cylinder based on accurate potential energy surfaces”. In: *Phys. Fluids* 33.5 (2021).

[16] Aram W Harrow, Avinatan Hassidim, and Seth Lloyd. “Quantum algorithm for linear systems of equations”. In: *Phys. Rev. Lett.* 103.15 (2009), p. 150502.

[17] Warren J Hehre, Robert F Stewart, and John A Pople. “Self-consistent molecular-orbital methods. I. Use of Gaussian expansions of Slater-type atomic orbitals”. In: *J. Chem. Phys.* 51.6 (1969), pp. 2657–2664.

[18] Robert Hellmann. “Ab initio potential energy surface for the nitrogen molecule pair and thermophysical properties of nitrogen gas”. In: *Mol. Phys.* 111.3 (2013), pp. 387–401.

[19] Adam A Holmes, Norm M Tubman, and CJ Umrigar. “Heat-bath configuration interaction: An efficient selected configuration interaction algorithm inspired by heat-bath sampling”. In: *J. Chem. Theory Comput.* 12.8 (2016), pp. 3674–3680.

[20] E-Wen Huang and Peter K Liaw. “High-temperature materials for structural applications: New perspectives on high-entropy alloys, bulk metallic glasses, and nanomaterials”. In: *MRS Bulletin* 44.11 (2019), pp. 847–853.

[21] *IBM Quantum Roadmap.* Accessed: 2025-02-21. URL: `https://www.ibm.com/quantum/technology#roadmap`.

[22] Pascual Jordan and Eugene Paul Wigner. *Über das paulische äquivalenzverbot.* Springer, 1993.

[23] Danil Kaliakin et al. “Accurate quantum-centric simulations of supramolecular interactions”. In: *ArXiv Preprint arXiv:2410.09209* (2024).

[24] Susheel Kumar, Krishna Murari Pandey, and Kaushal Kumar Sharma. “Recent developments in technological innovations in scramjet engines: A review”. In: *Mater. Today Proc.* 45 (2021), pp. 6874–6881.

[25] Matt Langione et al. “Quantum Computing Is Becoming Business Ready”. In: *Boston Consulting Group* 4 (2023).

[26] Xiangyu Li et al. “Potential quantum advantage for simulation of fluid dynamics”. In: *ArXiv Preprint arXiv:2303.16550* (2023).

[27] Ieva Liepuoniute et al. “Quantum-Centric Study of Methylene Singlet and Triplet States”. In: *arXiv preprint arXiv:2411.04827* (2024).

[28] Nadeem Fayaz Lone, Frank Czerwinski, and Daolun Chen. “Present challenges in development of lightweight high entropy alloys: A review”. In: *Appl. Mater. Today* 39 (2024), p. 102296.

[29] Pauline Ollitrault et al. “Quantum equation of motion for computing molecular excitation energies on a noisy quantum processor”. In: *Phys. Rev. Res.* 2 (Oct. 2020), p. 043140.

[30] Yuliya Paukku et al. “Global ab initio ground-state potential energy surface of N_4”. In: *J. Chem. Phys.* 139.4 (2013).

[31] John Penuel et al. “Feasibility of accelerating incompressible computational fluid dynamics simulations with fault-tolerant quantum computers”. In: *ArXiv Preprint arXiv:2406.06323* (2024).

[32] Alberto Peruzzo et al. “A variational eigenvalue solver on a photonic quantum processor”. In: *Nat. Commun.* 5.1 (2014), pp. 1–7.

[33] Adam B Peters et al. “Materials design for hypersonics”. In: *Nature communications* 15.1 (2024), p. 3328.

[34] Oded Regev. “An efficient quantum factoring algorithm”. In: *ArXiv Preprint arXiv:2308.06572* (2023).

[35] Julia Rice et al. “Quantum computation of dominant products in lithium–sulfur batteries”. In: *J. Chem. Phys.* 154 (Apr. 2021), p. 134115.

[36] Javier Robledo-Moreno et al. “Chemistry beyond exact solutions on a quantum-centric supercomputer”. In: *ArXiv Preprint arXiv:2405.05068* (2024).

[37] Manuel Salas. “A review of hypersonics aerodynamics, aerothermodynamics and plasmadynamics activities within NASA’s fundamental aeronautics program”. In: *39th AIAA Thermophys. Conf.* 2007, p. 4264.

[38] Luca Salasnich, Sauro Succi, and Adriano Tiribocchi. “Quantum wave representation of dissipative fluids”. In: *Int. J. Mod. Phys. C* 35.08 (2024), p. 2450100.

[39] Yuki Sato et al. “Quantum topology optimization of ground structures using noisy intermediate-scale quantum devices”. In: *arXiv preprint arXiv:2207.09181* (2022).

[40] Akhil Shajan et al. “Towards quantum-centric simulations of extended molecules: sample-based quantum diagonalization enhanced with density matrix embedding theory”. In: *ArXiv Preprint arXiv:2411.09 861* (2024).

[41] Sandeep Sharma et al. “Semistochastic heat-bath configuration interaction method: Selected configuration interaction with semistochastic perturbation theory”. In: *J. Chem. Theory Comput.* 13.4 (2017), pp. 1595–1604.

[42] Qiming Sun et al. “PySCF: the Python-based simulations of chemistry framework”. In: *WIREs Comput. Mol. Sci.* 8.1 (2018), e1340.

[43] Vikram Sundar. “Bounds on Errors in Observables Computed from Molecular Dynamics Simulations”. In: *Harvard University* (2018).

[44] Felix Tennie et al. “Quantum computing for nonlinear differential equations and turbulence”. In: *Nat. Rev. Phys.* (2025), pp. 1–11.

[45] The ffsim developers. *ffsim: Faster simulations of fermionic quantum circuits.* URL: `https://github.com/qiskit-community/ffsim`.

[46] Almudena Carrera Vazquez, Ralf Hiptmair, and Stefan Woerner. “Enhancing the quantum linear systems algorithm using Richardson extrapolation”. In: *TQC* 3.1 (2022), pp. 1–37.

[47] Wenqing Zhang et al. “A review of the mathematical modeling of equilibrium and nonequilibrium hypersonic flows”. In: *Adv. Aerodyn.* 4.1 (2022), p. 38.